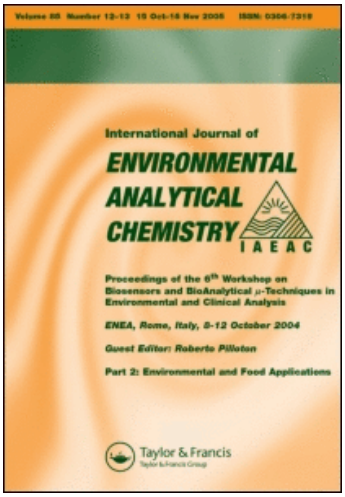

International Journal of Environmental Analytical Chemistry
Publication details, including instructions for authors and subscription information:
http://www.informaworld.com/smpp/title~content=t713640455

Laser Mass Spectrometry of Organophosphorus Pesticides and Related Compounds

John J. Morelli[a]; Somayajula K. Viswanadham[a]; Andrew. G. Sharkey JR.[a]; David M. Hercules[a]
[a] Department of Chemistry, University of Pittsburgh, Pittsburgh, PA, USA

To cite this Article Morelli, John J. , Viswanadham, Somayajula K. , Sharkey JR., Andrew. G. and Hercules, David M.(1987) 'Laser Mass Spectrometry of Organophosphorus Pesticides and Related Compounds', International Journal of Environmental Analytical Chemistry, 31: 2, 295 — 323
To link to this Article: DOI: 10.1080/03067318708077147
URL: http://dx.doi.org/10.1080/03067318708077147

Intern. J. Environ. Anal. Chem., Vol. 31, pp. 295–323
Photocopying permitted by license only

Printed in Great Britain

Laser Mass Spectrometry of Organophosphorus Pesticides and Related Compounds

JOHN J. MORELLI, SOMAYAJULA K. VISWANADHAM, ANDREW G. SHARKEY, JR. and DAVID M. HERCULES*

Department of Chemistry, University of Pittsburgh, Pittsburgh, PA 15260, USA

Dedicated to Professor W. Haerdi on the occasion of his 60th birthday

(*Received 10 June 1987; in final form 22 June 1987*)

Laser mass spectra obtained for 20 organophosphorus (OP) compounds were systematically evaluated for groups containing analogous structural features. Variations in fragmentation can be understood based on simple organic reactions. While detailed mechanistic interpretations of the laser mass spectra (LMS) were not possible, the qualitative features in the LMS obtained from five compounds, not in the original set, could be predicted based on the characteristics of the other OP compounds studied. The success of the prediction lends credence to the qualitative models developed for rationalizing the LMS. A specific feature in the LMS of aromatic thionophosphates is a thiono-thiolo rearrangement. Detailed investigation into the phenomena involved comparison of LMS obtained from aromatic thionophosphates with spectra from electron impact, chemical ionization, field desorption, and secondary ion mass spectrometry. These results led to the conclusion that the rearrangement in laser mass spectrometry must occur during volatilization while the molecule/ion is in the "cloud" present immediately above the laser impact area.

KEY WORDS: Organophosphorus compounds, laser MS, mass spectrometry, thionophosphates, SIMS.

*Author to whom correspondence should be addressed.

1. INTRODUCTION

Organophosphorus (OP) compounds represent a large portion of the agricultural chemicals used to protect crops and livestock from the detrimental effects of pests. OP pesticides have all but replaced organochlorine compounds which were found to be long-term contaminants in the food chain. OP pesticides undergo a variety of reactions, including hydrolysis and oxidation, forming end products with significantly reduced toxicity. These decomposition reactions limit the time OP pesticides interact with the environment; nevertheless, the short-term effects of OP pesticides are important.[1,2]

Gas chromatography is the primary analytical technique used to monitor hazardous compounds (including OP pesticides).[3] A more powerful tool is gas chromatography combined with mass spectrometry (GCMS);[1] however, GCMS techniques are limited to analyses of sample extracts, yielding data which reflect bulk concentration only. Information regarding the spatial distribution of OP pesticides on or within analytical samples cannot be obtained. Studying the spatial distribution of pesticides would increase the understanding of how these compounds interact within biological and environmental matrices. A recent report demonstrates that laser mass spectrometry (LMS) can be applied to studies of plant tissue surfaces containing pesticide residues.[4] While spatial information was not obtained in the preliminary study, the spatial resolution of the spectrometer employed ($\sim 5\,\mu$m) suggests that acquiring such information is feasible.

This report presents the LMS data obtained from OP pesticides and metabolites. A total of 25 compounds was investigated; the pesticides studied are representative of the OP compounds currently in use. The factors influencing the LMS features observed are discussed; some comparisons between LMS and previously obtained electron impact [EI],[5,6] chemical ionization [CI],[7,8] field desorption [FD],[9] and secondary ion [SIMS][10,11] mass spectra are presented. Characterizing the LMS of representative OP pesticides and their oxidation/hydrolysis products can aid future LMS investigations into the interaction of organic compounds within the environment.

2. EXPERIMENTAL

Laser mass spectra were obtained using a commercial laser micro-

probe mass spectrometer, the Leybold–Heraeus LAMMA-1000®. The instrument is described in detail elsewhere.[12] The ionization source consists of a Nd:YAG laser; the fundamental frequency (1060 nm) is quadrupled to 265 nm. The beam is Q-switched providing a pulse of 15 ns FWHM. The laser intensity can be varied continuously by a pair of twisted polarizers. The diameter of the laser at the focal point is approximately 5 μm. The laser beam impinges the sample at an angle of 45° to the surface. Samples are mounted on an x, y, z, micromanipulator having a maximum scanning range of 70 mm × 50 mm × 50 mm, respectively. The sample can be viewed by an optical microscope at a magnification of 250×, and the area of interest is positioned using the sample manipulator. Ions formed by interaction of the laser with the sample surface are extracted normal to the surface. These ions are accelerated (4 KV) into a time-of-flight (1.8 m flight length) mass spectrometer equipped with an ion reflector to compensate for the initial spread of ion kinetic energies. The ions are ultimately postaccelerated to 7 KV and detected by a Cu–Be secondary electron multiplier (Thorne–EMI model 964314A). The signal is amplified (10×) and fed into a Biomation 8100 transient recorder digitizing at 100 MHz. The digitized signal is temporarily stored in 2K bytes of transient recorder memory. The data are then displayed and/or transferred to disc storage using a Hewlett-Packard HP-1000 Series E computer. The spectral resolution (M/ΔM) of the instrument is 800 (FWHM) at m/z 350; however, resolution at constant reflector voltage depends on the incident laser energy, as well as the physical and chemical properties of the material analyzed.[13] No attempt was made to optimize the reflector voltage for each sample analyzed. Optimization for randomly selected samples resulted in a resolution increase of no more than a factor of four.

Spectra of all solid OP analytes were taken with the laser focused 5–50 μm in front of the sample surface (defocused mode). Estimated diameter of the impinging laser spot on the surface under these conditions is 8–10 μm. The laser energy was kept at $\sim 7\ \mu$J $\pm 20\%$, which represented 5–10 times the threshold laser power. Spectra reported in figures are single shot spectra representative of the data obtained under the predefined laser energy and focusing conditions. The relative intensities reported were obtained by averaging 6–8 indivdual spectra. Generally relative peak intensity variations were

± 30–55%; fragments showing less than 10% relative abundance varied as much as $\pm 100\%$.

OP compounds were obtained from the Environmental Protection Agency Repository, Research Triangle, NC.[14] The purity of each sample was reported to be 95–99%; 300 MHz proton NMR and gas chromatography were used for purity confirmation. Sample source independence of the mass spectra was determined by purchasing chlorpyrifos (compound **1**, purity 98%) and azinphos-methyl (compound **8**, purity 98.8%) from Chem Service, West Chester, PA, and comparing spectra obtained with those from the EPA samples. Zn foils were used as received. All reagents were of analytical grade and used without further purification.

Solid compounds were dissolved (0.4 μg of analyte) in methanol (solution concentration 40 mg/ml); subsequently, a 4 μl drop of the solution was placed on a $\sim 1\,cm^2$ area of Zn foil using a microsyringe. Several grains ($\sim 1\,mm^3$) of solid analyte were added to the drop preceding methanol evaporation. After the methanol was removed by air drying, the sample was mounted on the micromanipulator of the LAMMA-1000.

A general feature of both the positive and negative LMS obtained from most OP compounds studied was observation of intense signals in the region below $\sim$m/z 125. The resolution of the spectrometer makes unique structural assignment impossible for many of the ions observed (e.g., $[PO_2]^+$ and $[PS]^+$ have the same nominal mass). Furthermore, little specific information about the molecular structure of the pesticides can be derived from these low mass fragments. The factors presented above prompted time-delayed electronic signal acquisition and storage so that the structurally ambiguous low m/z region was not studied. This delay ($\sim 30\,\mu s$) varied with molecular weight and structure of the specific compound being analyzed. The mass range for which data were acquired was generally between m/z 125 and m/z 700; two or three separate laser shots were required.

Because of the limited 8-bit resolution of the transient recorder, digitizing spectra required two or three recorder sensitivities to ensure detection of weak signals while allowing full digitization of intense signals. The validity of the methodology was verified by splitting and diverting the signal to a second transient recorder allowing digitization of a spectrum from one laser shot at two input ranges. A Student t-test ($\alpha/2 = 0.05$) was used to compare digitization

of spectra resulting from two laser shots with that from one laser shot. No significant difference was found; however, splitting the signal from one laser shot is preferred due to the ease of data manipulation and elimination of possible sampling bias.

3. RESULTS AND DISCUSSION

The notation and nomenclature used is consistent with that of past reports on systematic mass spectrometric investigations of OP compounds.[5,7,9] This notation is based on the general formula I representative of the OP pesticides. The group Z can vary from small aliphatic chains to heterocyclic rings; the Z substituent may contain halogens, carboxylic acids, and amines. R_a and R_b normally refer to methyl, ethyl, or phenyl groups; X_{1-4} are oxygen or sulfur atoms. In some instances either of X_i ($i = 1$–3) may be absent.

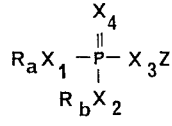

(I)

Tables 1–4 summarize the ions observed in the LMS of 20 OP pesticides. The pesticides are grouped according to structural similarities. Also shown is a number which references each compound for the purpose of subsequent discussion. The mass region sampled for positive or negative ion LMS is indicated. The ions observed for each compound (both positive and negative) are listed showing their m/z value, relative ion intensity (relative to the strongest signal obtained in the spectral region studied), and a notation indicating the ion type.

3.1 Fragmentation of halogenated and nitrated aromatic organophosphorus compounds

The first class of OP pesticides investigated (arbitrarily called Class I) contained halogenated or nitrated aromatic Z substituents. These

compounds were chlorpyrifos **1**, chlorpyrifos methyl **2**, chlorpyrifos OA **3** (**3** is the oxidation product of **1**), leptophos **4**, leptophos OA **5** (**5** is the oxidation product of **4**), EPN **6**, and bromophos **7**. Compounds **1–3** are structurally similar, as are compounds **4** and **5**. The overall structural variation between compounds **1–7** is well suited for exploring ion fragmentation and correlating the results with "chemical logic".

3.1.1 Positive ion spectra Figure 1 illustrates the positive ion LMS of bromophos. The spectrum was acquired at a laser energy of 7 μJ $\pm 20\%$. The spectrum presented in Figure 1 is a composite of two spectra obtained using different transient recorder settings. The details of the positive ion LMS of bromophos will be considered in turn below.

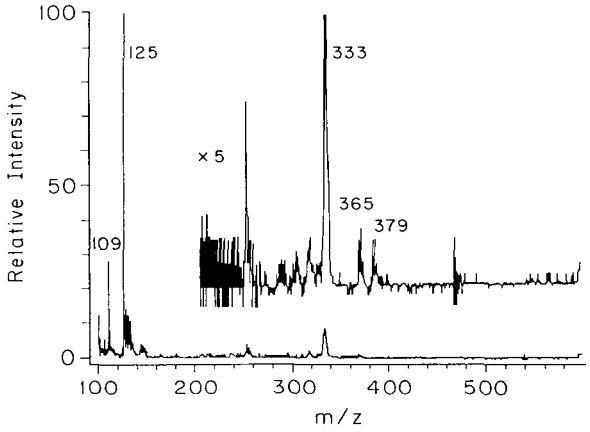

Figure 1 Positive ion LMS obtained from bromophos laser energy 7 μJ $\pm 20\%$.

Table 1 shows that the following ions appeared consistently in the positive laser mass spectra of the chlorpyrifos analogs: $[M+H]^+$; $[M-R]^+$; $[M-Cl]^+$; $[M-RO]^+$; $[M-OZ]^+$; $[M-SZ]^+$ (this ion did not occur for chlorpyrifos OA due to the absence of a sulfur atom); $[192]^+$ (no hypothetical structure exists at this time; however, the isotopic distribution indicates three chlorine atoms are present); $[OZ+2H]^+$; and $[SZ+2H]^+$ (the latter ion did not occur for chlorpyrifos OA due to the absence of a sulfur atom).

The relative intensities of the positive ions observed for compounds **1–3** show decreasing intensities for: $[M+H]^+$; $[M-R]^+$; $[M-Cl]^+$; $[192]^+$; and $[OZ-2H]^+$ in the order chlorpyrifos $\gg$ chlorpyrifos methyl $\geqq$ chlorpyrifos OA. The variation in relative ion intensities of $[M-RO]^+$, $[M-OZ]^+$, and $[M-SZ]^+$ between compounds **1–3** did not follow the above trend. The $[M-RO]^+$ intensities varied in order chlorpyrifos methyl $\gg$ chlorpyrifos $\geqq$ chlorpyrifos OA; $[M-OZ]^+$ varied as chlorpyrifos OA $\gg$ chlorpyrifos $\geqq$ chlorpyrifos methyl; $[M-SZ]^+$ did not vary between the two sulfur containing chlorpyrifos analogs (compounds **1** and **2**).

Compounds **4–6** are structurally similar; each is a phenyl phosphonate or thionophosphonate. Table 1 indicates that four common ions were seen for compounds **4**, **5**, and **6**: $[M-RO]^+$; $[M-OZ]^+$; $[PhPOH]^+$; and $[PhP]^+$ (Ph = phenyl). Another ten ions were specific to individual compounds or the thionophosphonates; many of these specific ions are characteristic of the structural differences between compounds **4–6** (e.g., EPN did not show $[M-Cl]^+$ due to the absence of a chlorine atom). The relative ion intensities of $[M-RO]^+$ varied in the order leptophos OA > leptophos > EPN; $[M-OZ]^+$ varied in the order EPN > leptophos > leptophos OA; $[PhPOH]^+$ varied in the order leptophos OA $\gg$ leptophos > EPN; $[PhP]^+$ did not vary significantly.

Bromophos **7** was investigated because of its structural similarities to compounds **1–5**. The **Z** substituent of bromophos is identical to leptophos; however, the alkyl thionophosphate moiety is similar to the chlorpyrifos analogs. The positive laser mass spectra of bromophos (Figure 1) showed six characteristic ions consistently: $[M+H]^+$, $[M+R]^+$, $[M-RO]^+$, $[M-Cl]^+$, $[M-OZ]^+$ and $[M-SZ]^+$.

Analyzing the fragmentation for compounds **1–7** provides insight into the LMS behavior of Class I OP pesticides. The relative intensities of $[M+H]^+$ for compounds **1–7** indicate that effective basicity is increased when: the alkyl group is C_2H_5 rather than CH_3; a hetero-nitrogen is present in the **Z** subsituent; and when $\mathbf{X_4}=\mathbf{S}$ ($\mathbf{X_4}$ corresponds to structure I). Comparing the relative ion intensities of $[M+H]^+$ and $[M+R]^+$ indicates that appearance of both ions depends on the **Z**, $\mathbf{R_a}$, and $\mathbf{R_b}$ substituents. When $[M+H]^+$ is strong, $[M+R]^+$ does not occur (compounds **1** and **6**); nor does $[M+R]^+$ occur for the remaining chlorpyrifos analogs (compounds **2** and **3**).

Table 1 Ions observed in LMS of OP pesticides containing halogen or nitro aromatics[a] (class I)

	Chlorpyrifos		*Chlorpyrifos methyl*		*Chlorpyrifos OA*		*Leptophos*		*Leptophos OA*		*EPN*		*Bromophos*	
Compound no.	**1**		**2**		**3**		**4**		**5**		**6**		**7**	
M.W.	349		321		333		410		394		323		364	
Mass range studied	*m/z* 130–700		*m/z* 105–700		*m/z* 150–700		*m/z* 105–1000		*m/z* 105–1000		*m/z* 105–1000		*m/z* 105–750	
Positive ions[b]	*Mass*	*Rel. int.*	*Mass*	*Rel. int.*	*Mass*	*Rel. int.*	*Mass*	*Rel. int.*	*Mass*	*Rel. int.*	*Mass*	*Rel. int.*	*Mass*	*Rel. int.*
M+H	350	64	322	8	334	2	411	5	395	0	324	17	365	2
$M+H-H_2S$	N/A		N/A		N/A		377	0	361	0	290	11	N/A	
M+R	378	0	336	0	362	0	425	5	409	25	352	0	379	2
M−R	320	30	306	2	304	2	395	0	379	0	294	12	349	0
M−R+2H	N/A		N/A		N/A		397	0	381	0	296	9	351	0
M−Z+2H	N/A		N/A		N/A		199	0	183	0	203	6	143	0
M−Cl	314	66	286	10	298	5	375	48	359	5	N/A		329	1
M−RO	304	20	290	100	288	6	379	5	363	30	278	10	333	20
M−OZ	153	20	125	10	137	100	171	100	155	35	185	100	125	100
M−SZ	137	10	109	10	N/A		155	32	N/A		169	53	109	16
c	192	20	192	10	192	3	N/A		N/A		N/A		N/A	
OZ+2H	198	100	198	30	198	5	N/A		N/A		N/A		N/A	
SZ+2H	214	4	214	2	N/A		N/A		N/A		N/A		N/A	
PhPOH	N/A		N/A		N/A		125	28	125	100	125	10	N/A	
PhPSH	N/A		N/A		N/A		141	72	N/A		141	63	N/A	
PhP	N/A		N/A		N/A		108	5	108	15	108	10	N/A	
$M-NO_2$	N/A		N/A		N/A		N/A		N/A		277	11	N/A	

Table 1 (continued)

Compound no.	**1**		**2**		**3**		**4**		**5**		**6**		**7**	
Mass range studied	*m/z* 160–700		*m/z* 140–700		*m/z* 150–700		*m/z* 180–1000		*m/z* 180–1000		*m/z* 130–1000		*m/z* 140–750	
Negative ions[b]	*Mass*	*Rel. int.*	*Mass*	*Rel. int.*	*Mass*	*Rel. int.*	*Mass*	*Rel. int.*	*Mass*	*Rel. int.*	*Mass*	*Rel. int.*	*Mass*	*Rel. int.*
M−H	348	5	320	0.5	332	0	409	100	393	33	322	5	363	0.5
M−H−HCl	312	2	284	10	296	100	373	12	357	9	N/A		327	10
M−H−HBr	N/A		N/A		N/A		329	16	313	18	N/A		283	0
M−R	320	22	306	50	304	100	N/A		N/A		N/A		349	50
M−Z	169	100	141	100	153	50	197	18	181	20	201	50	141	100
OZ	196	37	196	37	196	90	239	98	239	100	138	100	239	37
SZ	212	6	212	6	N/A		255	9	N/A		154	15	255	6

[a]Only fragments seen consistently from shot-to-shot are listed; intensities are relative to the most intense ion observed in the portion of the mass spectrum indicated. Relative standard deviations of intensity values reported are ±25%.

[b]**Z** and **R** correspond to the general structure I presented in text. Substrate employed was Zn.

[c]The structure of this ion has not been established; however, the isotopic distribution indicates that three chlorine atoms are present.

N/A. This ion not expected for this structure.

For all compounds: $X_2=X_3=0$; $X_1=0$ for **1**, **2**, **3**, **7** and is absent for **4**, **5**, **6**; $X_4=0$ for **3** and **5**; $X_4=S$ for **1**, **2**, **4**, **6**, **7**; $R_a=R_b=C_2H_5$ for **1** and **3**; $R_a=R_b=CH_3$ for **2** and **7**; $R_a=C_6H_5$ for **4**, **5**, **6**; $R_b=CH_3$ for **4**, **5**; and $R_b=C_2H_5$ for **6**. Z=(3,5,6-trichloro-2-pyridinyl) for **1**, **2**, **3**; (4-bromo,2,5-dichlorophenyl) for **4**, **5** and **7**; and Z=4-nitrophenyl for **6**.

The presence of $[SZ+2H]^+$ and $[OZ+2H]^+$ supports hetero-nitrogen protonation for chlorpyrifos analogs over other possible protonation sites. Chlorpyrifos analogs are the only Class I compounds which exhibit $[SZ+2H]^+$ and/or $[OZ+2H]^+$, suggesting that the hetero-nitrogen atom within the **Z** substituent is integral in producing these ions. Thus the following structures are proposed for $[M+H]^+$, $[SZ+2H]^+$, and $[OZ+2H]^+$ of chlorpyrifos:

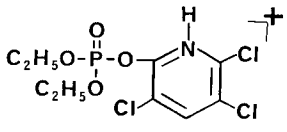

(II)

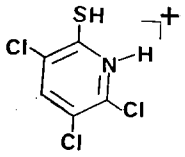

(III)

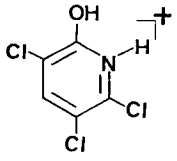

(IV)

Some fragment ions observed in the positive ion laser mass spectra of compounds **1–7** are structurally specific. For example, $[M-NO_2]^+$ requires the presence of NO_2. The intensities of $[M-OZ]^+$ relative to $[M-SZ]^+$, and the variation in base peaks among Class I compounds, will be discussed under the thiono-thiolo rearrangement.

3.1.2 Negative ion spectra Figure 2 shows the negative ion laser mass spectrum of chlorpyrifos; three shots were required to measure the intensities of all characteristic signals in the spectrum. Negative ion spectra of OP compounds generally showed poorer signal/noise than the corresponding positive ion spectra, possibly due to stray electrons generated by the pumping system of the time-of-flight analyzer.

The negative ion spectra of compounds **1–3** are characterized by six common fragment ions, as listed in Table 2: $[M-H]^-$; $[M-H-HCl]^-$; $[M-R]^-$; $[M-Z]^-$; $[OZ]^-$; and $[SZ]^-$. The $[SZ]^-$ ion was not observed for chlorpyrifos OA due to the absence of a sulfur atom. The relative intensities of $[M-H]^-$ varied in the order chlorpyrifos > chlorpyrifos methyl > chlorpyrifos OA; $[M-H-HCl]^-$ and $[M-R]^-$ relative ion intensities varied in the order chlorpyrifos OA > chlorpyrifos methyl > chlorpyrifos; $[M-Z]^-$ relative ion intensities varied as chlorpyrifos > chlorpyrifos methyl > chlorpyrifos OA; $[OZ]^-$ varied as chlorpyrifos OA > chlorpyrifos > chlorpyrifos methyl; $[SZ]^-$ showed no variation between chlorpyrifos and chlorpyrifos methyl.

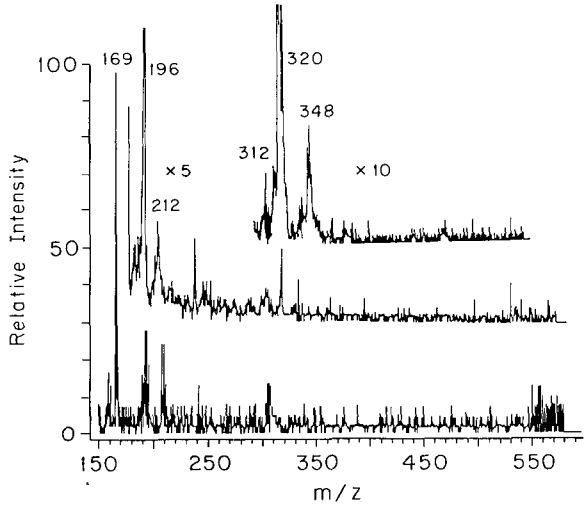

Figure 2 Negative ion LMS obtained from chlorpyrifos laser energy 7 μJ $\pm$ 20%.

The negative ion LMS of compounds **4–6** were characterized by $[M-H]^-$, $[OZ]^-$, and $[M-Z]^-$. Ions $[M-H-HBr]^-$ and $[M-H-HCl]^-$ did not occur in the LMS of EPN due to the absence of bromine and chlorine atoms; however, both ions were observed in the LMS of compounds **4–5**. No $[SZ]^-$ ions were observed in the LMS of leptophos OA due to the absence of a sulfur atom. The relative ion intensity of $[M-H]^-$ varied in the order leptophos > leptophos OA > EPN; $[M-H-HBr]^-$ and $[M-H-HCl]^-$ did not vary significantly between the leptophos analogs, and $[OZ]^-$ did not vary significantly between compounds **4–6**. $[SZ]^-$ did not vary significantly between leptophos and EPN. Note that $[SZ]^-$ is not expected for leptophos OA since this compound is not a thionophosphate. The $[M-Z]^-$ intensity varied as EPN > leptophos > leptophos OA.

The negative ion laser mass spectra of bromophos showed six ions: $[M-H]^-$, $[M-H-HCl]^-$, $[M-R]^-$, $[M-Z]^-$, and $[OZ]^-$, $[SZ]^-$. The structural similarities of bromophos to the chlorpyrifos analogs **1** and **2** (similar alkyl thionophosphate moieties) and the leptophos analogs (identical **Z** substituents) aid in understanding the effect of structure on the negative ion LMS of Class I compounds.

Table 2 Ions observed in LMS of OP pesticides having hetero-nitrogen ring systems without halogens[a] (class II)

	Azinphos-methyl		*Azinphos-ethyl*		*Phosmet*		*Phosmet OA*		*Ditalimphos*		*Pyrazophos*	
Compound no.	**8**		**9**		**10**		**11**		**12**		**13**	
M.W.	317		345		317		301		299		373	
Mass range studied	*m/z* 120–700		*m/z* 130–700		*m/z* 100–700		*m/z* 100–700		*m/z* 100–700		*m/z* 135–750	
Positive ions[b]	*Mass*	*Rel. int.*	*Mass*	*Rel. int.*	*Mass*	*Rel. int.*	*Mass*	*Rel. int.*	*Mass*	*Rel. int.*	*Mass*	*Rel. int.*
M+H	318	0	346	1	318	0	302	1	300	80	374	15
M+H−CO		N/A		N/A	290	0	274	0	272	90		N/A
M+H−2CO		N/A		N/A	262	0.5	246	0	244	95		N/A
M+R	332	0	374	0	332	5	316	0	328	0	402	5
M+Z	477	4	505	0	477	20	461	3	445	0	577	0
M+Z−CO	449	5	477	5		N/A		N/A		N/A		N/A
M−R	302	0	316	0		N/A		N/A		N/A	344	0
M−RO	286	24	300	25	286	0	270	0	254	0	328	0
M−SZ[c]	125	10	153	15	125	5	109	1		N/A	137	15
M−NZ		N/A		N/A		N/A		N/A	153	1		N/A
Z	160	15	160	15	160	100	160	100	146	0	204	0
Z+2H		N/A		N/A	162	0	162	0	148	90	206	0
Z+2H−H_2O		N/A		N/A	144	0	144	0	130	100		N/A
Z−CO	132	100	132	100		N/A		N/A		N/A		N/A
OZ+2H		N/A		N/A		N/A		N/A		N/A	222	100

	Azinphos-methyl		*Azinphos-ethyl*		*Phosmet*		*Phosmet OA*		*Ditalimphos*		*Pyrazophos*	
Compound no.	**8**		**9**		**10**		**11**		**12**		**13**	
SZ+2H[c]	194	0	194	0	N/A		N/A		N/A		238	1
PhCNH	N/A		N/A		103	1	103	1	103	5	N/A	
M−OZ	N/A		N/A		N/A		N/A		N/A		153	50
Mass range studied	*m/z* 140–700		*m/z* 140–700		*m/z* 140–700		*m/z* 140–700		*m/z* 140–700		*m/z* 165–750	
Negative ions[b]	*Mass*	*Rel. int.*	*Mass*	*Rel. int.*	*Mass*	*Rel. int.*	*Mass*	*Rel. int.*	*Mass*	*Rel. int.*	*Mass*	*Rel. int.*
M−H	316	0	344	0	316	0.5	300	1	298	100	372	10
$M-CH_3$	N/A		N/A		N/A		N/A		N/A		358	5
$M-CO_2C_2H_5$	N/A		N/A		N/A		N/A		N/A		300	80
M−R	302	12	316	13	302	1	286	0	304	5	344	1
M−Z[d]	157	100	185	100	157	100	141	100	167	0	169	5
Z	160	0	160	0	160	0	160	0	132	0	204	100
$Z-CH_2$	146	10	146	10	N/A		N/A		N/A		N/A	
OZ	N/A		N/A		N/A		177	0	N/A		200	90
SZ	192	0	192	0	193	0	193	0	N/A		236	9
NZ or $Z-CH_2$[d]	N/A		N/A		146	10	146	10	146	50	N/A	

[a]Only ions seen consistently from shot-to-shot are listed; intensities are relative to the most intense peak in the portion of the mass spectrum indicated. Relative standard deviation of intensity values is ±25%.

[b]**Z** and **R** correspond to the general structure I presented in text. Substrate employed was Zn.

[c]Compounds **8** and **9** are dithiophosphates; therefore, M−OZ, OZ+2H and OZ are not expected.

[d]$Z-CH_2$ for phosmet and phosmet OA is the same fragment as NZ for ditalimphos ($C_8H_4O_2N$).

For all compounds $X_1=X_2=0$. For **8–10**, $X_3=X_4=S$; for **11**, $X_3=X_4=0$; for **12, 13**, $X_4=S$; X_3=absent for **12**; $X_3=0$ for **13**.

For **8, 10, 11**, $R_a=R_b=CH_3$; **9, 12, 13**, $R_a=R_b=C_2H_5$.

Z= 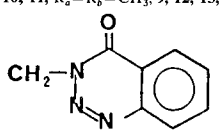 for **8, 9**; Z= 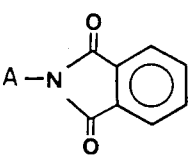 for **10–12**;

A=CH_2 for **10, 11** absent from **12**. 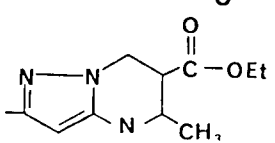 for **13**.

The $[M-R]^-$ ion intensities for compounds **1–7** depend on the **Z** substituent. Alternatively, $[M-H]^-$ ion intensities of compounds **1–7** depend on the presence of ethyl vs. methyl at one of the **R** sites. The negative ion LMS of compounds **1–7** show "chemically correct" trends. The intensity of $[M-H]^-$ for Class I compounds is low with the exception of the leptophos analogs (compounds **3** and **4**). The enhancement of $[M-H]^-$ in the negative ion LMS of Class I compounds containing a phenyl moiety α to phosphorus can be rationalized by increased resonance stabilization by the α moiety. The apparent preference of $[M-H]^-$ production in Class I compounds having $\mathbf{X}_4=S$ vs. $\mathbf{X}_4=0$ can be attributed to an inductive effect. The surprisingly low production of $[M-H]^-$ for EPN is unclear at this time; however, it is likely that $[M-H]^-$ is formed (EPN also contains an α-phenyl group) but quickly fragments.

Production of $[M-H-HCl]^-$ in compounds **1–7** is straightforward; isotopic abundance confirms that one chlorine atom is eliminated. For compounds **1–3** production of $[M-H-HCl]^-$ must involve the loss of at least one alkyl proton. The most reasonable route to $[M-H-HCl]^-$ involves elimination of HCl. To eliminate HCl from chlorpyrifos methyl via loss of a second alkyl proton would require formation of a strained four member ring. Thus the loss of one aryl proton seems reasonable. The stability of CH_2 vs. C_2H_4[15] relates to the increased intensity of $[M-H-HCl]^-$ for chlorpyrifos methyl over chlorpyrifos. Chlorpyrifos OA shows intense $[M-H-HCl]^-$ relative to compounds **1** and **2** because the inductive effects of oxygen at the $\mathbf{X}_4$ site are significant.

For leptophos and leptophos OA formation of $[M-H-HX]^-$ (X = Cl, Br) does not necessarily require the loss of an alkyl proton. Rather, the phenyl group α to phosphorus is a likely source of one proton.

Compounds **4**, **5**, and **7** can lose either of two chlorines or a bromine. The competitive loss involving either Cl or Br atoms explains why the intensity of $[M-H-HCl]^-$ is not considerably greater than that observed for compounds **1–3**. March[15] states that benzyne production is favored by Br substitution relative to Cl. Production of $[M-H-HBr]^-$ is equal to or slightly higher than $[M-H-HCl]^-$ despite the statistically favored losses involving chlorine. The $[M-H-HBr]^-$ relative ion abundance, when compared to $[M-H-HCl]^-$, supports benzyne production. Note that

$[M-H-HCl]^-$ does not vary significantly between leptophos and leptophos OA (i.e., $\mathbf{X}_4$=sulfur or oxygen, respectively); this is consistent with resonance stabilized anions.

3.2 Fragmentation of organophosphorus compounds having hetero-nitrogen ring systems

Class II OP pesticides containing **Z** substituents with ring systems having at least one hetero-nitrogen atom. These compounds are azinphos-methyl **8**, azinphos-ethyl **9**, phosmet **10**, phosmet OA **11** (**11** is the oxidation product of **10**), ditalimphos **12**, and pyrazophos **13**. Compounds **8** and **9** are structurally similar, as are compounds **10–12**. A summary of LMS data for compounds **8–13** is given in Table 2.

3.2.1 Positive ion spectra The positive ion LMS for compounds **8–9** are characterized by an intense $[Z-CO]^+$ peak at m/z 132 (see Table 2). Neither compound shows $[M+H]^+$ or $[M+R]^+$; $[M+Z-CO]^+$ is seen in the LMS of both, and $[M+Z]^+$ is also seen for azinphos-methyl. These ions suggest that **Z** substituent ion-addition competes with formation of $[M+H]^+$ and $[M+R]^+$. Furthermore, "Z-type addition" is likely in cases where the **Z** substituent yields a dramatically stable ion. We have not determined whether **Z**-type additions involve ion-molecule reactions or some alternate associative process.

The intensity variation of $[M+H]^+$ between compounds **10–13** is further evidence that $\mathbf{R}_{a,b}=C_2H_5$ is important for producing a protonated quasimolecular species. Neither methyl ester shows intense $[M+H]^+$ in their positive ion LMS. The positive ion LMS of compounds **10–12** shows some similarities to those of compounds **8** and **9**. The base peaks for compounds **8–12** involve **Z**-type fragments. The phosmet analogs also show **Z**-type additions (i.e., $[M+Z]^+$) similar to the azinphos analogs. The presence of $\mathbf{X}_4$=S appears to dramatically influence the intensity of $[M+Z]^+$. Phosmet yields a much more intense $[M+Z]^+$ ion than its oxygen analog. The decreased $[M+Z]^+$ intensity when $\mathbf{X}_4$=0 may be due to closer proximity of the added **Z** substituent to the remainder of the molecule.

Compounds **12** and **13** are somewhat similar to the chlorpyrifos analogs; protonation is at a hetero-nitrogen position within the **Z** substituent ($[Z+2H]^+$ and $[Z+2H-H_2O]^+$ for ditalimphos; $[OZ+2H]^+$ and $[SZ+2H]^+$ for pyrazophos and the chlorpyrifos analogs). The presence of these ions is further evidence of the effect of hetero-nitrogens on $[M+H]^+$ production. The structure suggested for the fragment noted as $[Z+2H-H_2O]^+$ is:

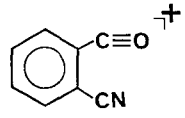

(V)

Production of $[M+H-CO]^+$ and $[M+H-2CO]^+$ is greater in the positive ion LMS of ditalimphos than the phosmet analogs.

3.2.2 Negative ion spectra The spectra of compounds **8–13** are characterized by intense $[M-Z]^-$ peaks. Compounds **8–11** showed $[Z-CH_2]^-$. Each Class II compound yielded $[M-R]^-$, except for phosmet OA. Compounds **10–13** show $[M-H]^-$; however, the methyl esters (**10** and **11**) yielded very low abundances of this ion. The negative ion LMS of ditalimphos contained $[Z]^-$, and pyrazophos yielded $[OZ]^-$, $[SZ]^-$, and $[Z]^-$ ($\mathbf{X}_3$ is absent from the structure of ditalimphos). The $[Z]^-$ ion seen in the negative ion LMS of ditalimphos is identical to the $[Z-CH_2]^-$ ion of the phosmet analogs.

The appearance of $[M-H]^-$ in Class II compounds correlates well with $[M+H]^+$ production. The presence of $\mathbf{R}_{a,b}=C_2H_5$ promotes production of both $[M+H]^+$ and $[M-H]^-$ ions in the LMS of Class II compounds.

Unlike Class I compounds, pyrazophos seems to favor formation of $[Z]^-$ relative to $[OZ]^-$. This may indicate that the $[OZ]^-$ fragment ion from pyrazophos is less stable than the $[OZ]^-$ phenolates of Class I compounds; however, it is more likely that this result reflects the strengths of the bonds breaking to produce $[Z]^-$ and $[OZ]^-$. Factors influencing bond strengths will be addressed when variations of $[OZ]^-$, $[SZ]^-$, $[M-OZ]^+$, and $[M-SZ]^+$ are considered (*vide infra*).

Both positive and negative ion LMS of compounds **8–11** indicate that fragmentation primarily involves cleavage at the X_3–CH_2 bond. The positive ion base peaks of compounds **8–11** are due to either the intact **Z** substituent or CO loss from the substituent.

3.3 Fragmentation of phosphoramid(othio)ic acid esters

The third class of compounds investigated were the phosphoramid(othio)ic acid esters: acephate **14**, crufomate **15**, and phosfolan **16**. Detailed comparison of fragmentation within Class III compounds is not possible due to the diverse structures of this small sample set; however, fragmentation of Class III compounds can be compared with the previous 13 compounds; the data are presented in Table 3.

3.3.1 Positive ion spectra The positive ion LMS of phosphoramid(othio)ic acid esters (Table 3) show a correlation between $[M+H]^+$ and $[M-H]^-$ production similar to that seen in Class II compounds. However, acephate is the first methyl ester studied to yield an intense $[M+H]^+$ in the positive ion LMS. This result can be understood by considering that the acetyl group is a proton source and may be responsible for increasing the overall basicity of acephate. Note that crufomate is a methyl ester which contains an $-NH-$ functionality; however, it does not yield $[M+H]^+$ or $[M-H]^-$. The $[M+H]^+$ of acephate may have added stability due to intramolecular hydrogen bonding.

The $[M+H]^+$ abundances of crufomate and phosfolan are typical of results obtained for compounds **1–13**. Crufomate, a methyl ester, did not show $[M+H]^+$; phosfolan, an ethyl ester, yielded $[M+H]^+$ as base peak. The positive ion LMS of acephate also showed: $[M+H-CO]^+$; $[M-R]^+$; $[M-Z]^+$; $[M-Z+2H]^+$; and $[M-Z]^+$. Crufomate yielded: $[M+R]^+$, $[M-Cl]^+$, $[M-RO]^+$, and $[M-OZ]^+$. The intense $[M+\widetilde{R}]^+$ observed in the positive ion LMS of crufomate is further evidence that competition between $[M+R]^+$ and $[M+H]^+$ formation exists. Crufomate has a source of methyl moieties external to the phosphoramidate kernel. The positive ion LMS of phosfolan showed $[M+H]^+$ (previously discussed), a weak $[M+R]^+$, $[M+H-C_2H_4]^+$, and $[M-Z]^+$. The loss of ethylene

Table 3 Fragments observed in LMS of phosphoramid(othio)ic acid esters[a,b] (class III)

	Acephate		*Crufomate*		*Phosfolan*	
Compound no.	**14**		**15**		**16**	
M.W.	183		291		255	
Mass range studied	m/z 120–400		*m/z* 105–600		*m/z* 115–550	
Positive ions	*Mass*	*Rel. int.*	*Mass*	*Rel. int.*	*Mass*	*Rel. int.*
M+H	184	54	292	0	256	100
M+H−CO	156	20	N/A		N/A	
M+R	198	0	316	95	284	10
M−R	168	8	376	0	226	0
M+H−C_2H_4	N/A		N/A		228	10
M−Cl	N/A		256	19	N/A	
M−RO	152	0	260	100	210	0
M−Z[a]	140	56	124	0	151	0
M−Z+2H	142	100	126	0	153	0
M−NZ or M−NHZ	125	34	N/A		137	3
M−OZ	N/A		108	97	N/A	
Mass range studied	*m/z* 130–400		*m/z* 120–600		*m/z* 150–525	
Negative ions	*Mass*	*Rel. int.*	*Mass*	*Rel. int.*	*Mass*	*Rel. int.*
M−H	182	52	290	0	254	100
M−H−HCl	N/A		254	0	N/A	
M−R	168	87	276	3	226[c]	90
M+OR	214	0	322	0	300	82
M−Z	140	100	124	9	151	0
OZ	N/A		183	100	N/A	

[a]Only ions seen consistently from shot-to-shot are listed; intensities are relative to the most intense peak observed in the spectral region indicated. Relative standard deviation of intensities is ±25%.

[b]**Z** and **R** correspond to general structure I. Substrate employed was Zn.

[c]This fragment may be due to either M−R or M−H−C_2H_4. See text for details.

N/A. Ion not expected for this structure.

$X_2=X_4=0$ for all compounds. X_1=S, absent, 0; X_3=absent, 0, absent for **14**, **15**, **16**, respectively. $R_a=R_b=CH_3$ for **14**; $R_a=R_b=C_2H_5$ for **16**; Ra=$NHCH_3$, Rb=CH_3 for **15**. Z=$NHCOCH_3$ for **14**, 2-chloro,4-5-butyl for **15**.

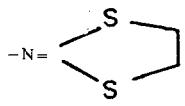

for 16.

from phosfolan is likely due to a rearrangement within the **Z** substituent:

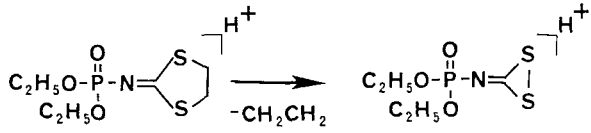

3.3.2 Negative ion spectra The intensity of $[M-H]^-$ in the negative ion LMS of acephate can be understood by considering that abstraction of a proton from the acetyl or amino moiety produces a resonance stabilized negative ion. Proton loss from the methyl (thio)ester of acephate is unlikely. Excluding the leptophos analogs, no methyl esters show significant $[M-H]^-$.

The negative ion LMS of crufomate show $[M-R]^-$, $[M-Z]^-$, and $[OZ]^-$. The abundance of $[OZ]^-$ reflects the stability of the phenolate ion. Phosfolan, an ethyl ester, shows $[M-H]^-$ as base peak in the negative ion LMS. Also seen are $[M+OR]^-$ and $[M-R]^-$, and/or $[M-H-C_2H_4]^-$. The elimination of ethylene observed in the positive ion LMS of phosfolan makes assigning the ion observed at m/z 226 difficult. Both $[M-R]^-$ and $[M-H-C_2H_4]^-$ would produce structurally different ions with identical masses; however, $[M-H-C_2H_4]^-$ would result in a strained three member ring involving a weak disulfide bond. The frequency of $[M-R]^-$ in the LMS of OP compounds makes $[M-R]^-$ the likely origin of m/z 226.

3.4 Fragmentation of potassium metabolite salts

The final class of compounds investigated contained four potassium salts of OP pesticides: KDEDTP **17**, KDETP **18**, KDMDTP **19**, and KDMTP **20**. The analytical importance of potassium metabolite salts of OP pesticides prompted LMS investigation of Class IV compounds. Table 4 lists the ions observed in the positive and negative ion LMS of compounds **17–20**. The ion intensities reported are relative to the most intense ion from the potassium salt studied.

3.4.1 Positive ion spectra The positive ion spectra of compounds **17–20** were relatively simple and dominated by an intense K^+ signal

Table 4 Ions observed in LMS of potassium salt metabolites[a] (class IV)

	KDEDTP		*KDETP*		*KDMDTP*		*KDMTP*	
Compound no.	**17**		**18**		**19**		**20**	
M.W.	224		208		196		180	
Mass range studied	*m/z* 125–450		*m/z* 125–425		*m/z* 125–400		*m/z* 100–400	
Positive ions	*Mass*	*Rel. int.*	*Mass*	*Rel. int.*	*Mass*	*Rel. int.*	*Mass*	*Rel. int.*
K	39, 41	100	39, 41	100	39, 41	100	39, 41	100
M−SK	153	3	137	4	125	2	109	4
M−OK	N/A		153	5	N/A		125	5
Mass range studied	*m/z* 125–450		*m/z* 125–425		*m/z* 125–400		*m/z* 100–400	
Negative ions	*Mass*	*Rel. int.*	*Mass*	*Rel. int.*	*Mass*	*Rel. int.*	*Mass*	*Rel. int.*
M−K	185	100	169	100	157	100	141	100
M−K−R	156	15	140	20	142	18	126	20

[a]Only fragments seen consistently from shot-to-shot are listed; intensities are relative to the most intense ion observed in the portion of the mass spectrum indicated. Relative standard deviation of reported intensity values is ±25%.
N/A. This ion not expected for this structure.

giving peaks at m/z 39,41. The phosphorodithioates (compounds **17** and **19**) show one other ion in their positive ion LMS: $[M-SK]^+$. The phosphorothioates (compounds **18** and **20**) each show two additional ions: $[M-SK]^+$ and $[M-OK]^+$.

3.4.2 Negative ion spectra The negative ion LMS of Class IV compounds contain a single peak in the indicated mass range (see Table 1): $[M-K]^-$. The presence of only $[M-K]^-$ in combination with the intense K^+ observed in the positive ion LMS of Class IV compounds indicates that the dominant ionization mechanism of Class IV compounds involves crystal lattice disruption.

3.5 Thiono–thiolo rearrangement

Many thionophosphates undergo isomerization to form thiolo-

phosphates:[16]

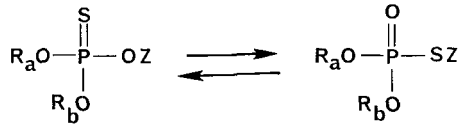

This isomerization is referred to as the thiono–thiolo rearrangement.[17,18] The thiono isomers are more stable at room temperature; however, formation of the thiolo isomer has been observed in many cases at elevated temperatures;[16] the rate of isomerization is first order.

The LMS of aromatic thionophosphates (compounds **1**, **2**, **4**, **6**, **7**, and **13**) show ions resulting from possible thiono–thiolo rearrangements: $[SZ]^-$; $[M-SZ]^+$; and in some spectra $[SZ+2H]^+$. The LMS obtained from aromatic thionophosphates were compared to spectra obtained from electron impact (EI), chemical ionization (CI), secondary ion (SIMS), and field desorption (FD) mass spectrometry.[5-11] Table 5 shows the average values for [Thiolo]/[Thiono] obtained by the various techniques. The information gained from this comparative study provided insight into the processes influencing formation of rearrangement fragment ions by each technique.

To determine whether thiono–thiolo rearrangement occurred prior to laser volatilization, the LMS of aromatic thionophosphate esters were studied at ambient and liquid nitrogen temperatures using a cold probe.[19] Studies of OP compounds at elevated temperatures was not possible due to sample volatility. No difference was observed in spectra obtained from liquid nitrogen cooled samples

Table 5 Thiolo fragment intensity relative to thiono fragment intensity as observed in EI, CI, FD, LMS, and SIMS.[a]

	Mass spectrometric technique				
	EI	*CI*	*FD*	*LMS*	*SIMS*
[Thiolo]/[Thiono]	0.3 ± 0.1[b]	>20	0	0.16 ± 0.06[b]	0.014 ± 0.004[b]

[a]EI = Electron impact mass spectrometry; CI = Chemical ionization mass spectrometry; FD = Field desorption mass spectrometry; LMS = Laser mass spectrometry; SIMS = Secondary ion mass spectrometry.

[b]Values are $\pm t(a, df)s_t N^{-1/2}$; $t(a/2, df)$ is Student-t critical value at confidence $(a/2)$ and degrees of freedom (df); s_t = standard deviation; N = Number of samples; $a/2 = 0.05$.

compared to ambient temperature. This result suggests that the low intensity rearrangement ions observed in LMS are not formed prior to volatilization. Sample impurity was also eliminated as a possible contributing factor to the $[SZ]^-/[OZ]^-$ ratio for LMS. The reported purity of 95–99% was confirmed with 300 MHz proton NMR and gas chromatography; no indication of thiolophosphate isomers was found. These results lead us to conclude that rearrangement must occur during volatilization while the molecule/ion is in the "cloud" immediately above the laser impact area.[20] The conditions of this area (including temperature) are governed by laser parameters (e.g., power density and pulse duration).[21] Studying the LMS of the OP compounds as a function of power density is not possible at present. The laser power needed to produce the phenolate, thiophenolate, and other ions of interest is within 30% of the maximum power output of our system, and the reproducibility of the important ions is 30–55% (weaker peaks have poorer reproducibility). The relative standard deviation of shot-to-shot laser energy is 20%. Instrumentation does not permit variation in laser pulse width.

Stan *et al.* report that rearrangement occurs after primary electron attachment in CI,[7] and the dependence of the $[SZ]^-/[OZ]^-$ ratio on temperature[7] correlates with the reported stability of some thiolo isomers.[16] This suggests that $[SZ]^-/[OZ]^-$ values depend on efficient thermal transfer to the ion. The thiono–thiolo rearrangement has been established for EI fragmentation of cyclic thionophosphate esters;[22] however, thermal transfers are not efficient.[23] The value of $[SZ]+H]^+/[OZ+H]^+$, measured by EI, is 0.3 for aromatic thionophosphates (Table 5). Further evidence supporting ionization prior to rearrangement is indicated by the $[SZ]^+/[OZ]^+$ ratio in FD. The short lifetimes of pre-extracted ions in FD[24] makes thermal transfers to ions unlikely in FD, resulting in no production of rearrangement ions. All evidence obtained to date indicates ionization preceeds rearrangement, and the $[SZ/OZ]^-$ ratio depends on efficient thermal transfer to the parent ion. We must, therefore, conclude that in LMS thermal transfers are not more efficient than those in EI; however, such transfers proceed in both EI and LMS.

The effective bond strength under laser ionization between phosphorus and the $\mathbf{X}_3$ oxygen (α to the **Z** substituent) can be compared to the effective bond strength of oxygen and the **Z** substituent by comparing $[M-Z]^-$ relative ion intensities to those of $[OZ]^-$. The

sulfur analogs of chlorpyrifos show significantly higher production of $[M-Z]^-$ relative to chlorpyrifos OA. This observation can be understood by considering the competition between $[OZ]^-$ and $[SZ]^-$ production which requires rearrangement of the thionophosphate to a thiolophosphate;[16] this rearrangement effectively increases the strength of the oxygen–phosphorus bond (the $\mathbf{X}_3$ oxygen). Chlorpyrifos OA does not have a sulfur atom at the $\mathbf{X}_4$ position; thus, any rearrangement of the phosphate would result in an identical structure and no stabilization of the oxygen–phosphorus bond. The stabilization due to thiono–thiolo rearrangement arises from the thermodynamic stability of the thiolo form at elevated temperatures.[16]

Leptophos, leptophos OA, and EPN show significantly higher $[OZ]^-$ production compared to other Class I compounds. The increase in $[OZ]^-$ ion intensity can be understood by considering the resonance stabilized cation resulting from the loss of $[OZ]^-$;

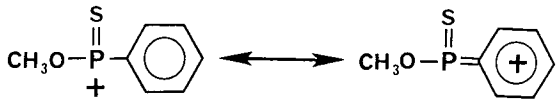

Resonance stabilization of the cation ($[M-OZ]^+$) produced after loss of $[OZ]^-$ explains the increased intensity of $[OZ]^-$ observed in the negative ion LMS of phenyl (thiono)phosphonates relative to spectra of alkyl (thiono)phosphates.

3.6 Prediction of spectra

Investigation of the 20 compounds reported here has provided insight into structural influences on LMS. The goal of such an investigation is to facilitate interpretation of mass spectra. A measure of its success is predictability. Specifically, how well can one estimate the LMS of OP compounds not previously studied? To address this question five additional OP pesticides were obtained. The LMS of each was predicted based on structural similarities to compounds **1–20**. The estimated spectrum was compared to the actual LMS for evaluation.

3.6.1 Predicative procedure The five additional compounds studied were coumaphos, **21,** iodofenphos **22**, ronnel **23**, dialifor **24**, and phosalone **25**. Table 6 presents the predicted and observed ions in the mass range studied; only ions observed consistently are reported. A Student-*t* test ($\alpha/2=0.005$) was used to determine the significance of differences between predicted and actual intensities. Significant intensity differences are highlighted with a superior "c" in Table 6.

The first step in predicting the LMS of compounds **21–25** was to make structural comparisons between these five pesticides and compounds **1–20**. Coumaphos was classified as a Class I compound (**Z** contained a halogenated aromatic compound); however, some dissimilarities exist. The halogen moiety is not directly bound to an aromatic position. Also, the presence of a cyclic carboxylic anhydride had to be accounted for. The ions likely to form, based on the spectra of other Class I compounds, were: $[M+H]^+$; $[M-R]^+$; $[M-Cl]^+$; $[M-OR]^+$; $[M-OZ]^+$; $[M-SZ]^+$; $[OZ+2H]^+$; $[SZ+2H]^+$; $[M-H]^-$; $[M-H-HCl]^-$; $[M-R]^-$; $[M-Z]^-$; $[OZ]^-$; and $[SZ]^-$. $[M+H]^+$ was justified based on the presence of $\mathbf{R}_{a,b}=C_2H_5$. The hetero-oxygen was assumed to behave similarly to a hetero-nitrogen, promoting production of $[OZ+2H]^+$ and $[SZ+2H]^+$. The appearance of the remaining ion was predicted from data for chlorpyrifos **1**. The peak at m/z 192 was not included because coumaphos does not have the three chlorines necessary. The intensities assigned to the predicted ions were based on chlorpyrifos.

Iodofenphos **22** and ronnel **23** were treated together because they have thionophosphate moieties like chlorpyrifos methyl and bromophos; therefore, $[M+H]^+$ and $[M-H]^+$ intensities should be minimal. Iodofenphos and ronnel have **Z** substituents similar to bromophos. Iodofenphos has an iodine atom replacing bromine; ronnel has an added chlorine atom replacing bromine. The ions that occurred in bromophos were predicted to appear in the LMS of both iodofenphos and ronnel; however, $[M-H-HBr]^-$ was replaced by $[M-H-HI]^-$ for iodofenphos and $[M-H-HBr]^-$ was eliminated from the list of predicted fragments for ronnel. To test the proposal that formation of $[M-H-HY]^-$ (Y=halogen) involved benzyne production, we predicted that $[M-H-HI]^-$ would have greater intensity than $[M-H-HCl]^-$ in the negative ion spectra of iodofenphos.[15] $[M-I]^+$ was not expected for iodofenphos due to the absence of $[M-Br]^+$ in the positive ion LMS of bromophos.

Dialifor and phosalone were classified as Class II compounds. Each was expected to yield intense $[Z]^+$ ions or fragment ions. Dialifor and phosalone were also expected to exhibit **Z** type additions in their positive ion LMS. An $[M+H]^+$ ion was not expected for these compounds; however, $[M-H]^-$ was expected with an intensity $\leq 1\%$ of base peak (based on the performance of phosmet). The remaining ions and intensity predictions for dialifor and phosalone were based on data for phosmet.

3.6.2 Accuracy of prediction Generally the predictions were accurate within the reproducibility of the relative peak intensity measurements (± 33–55%); however, one ion appeared in the spectrum of coumaphos which was not predicted $[M-H-CH_3Cl]^-$. The unpredicted fragment is attributable to the presence of a moiety not represented in the data set sampled (compounds **1**–**20**). Some intensity predictions were inaccurate. For example, ronnel **23** showed a strong $[M+R]^+$ ion, while a much lower value was predicted based on bromophos. Inaccurate intensity predictions are attributable to insufficient functional group representation in the data base employed (twenty compounds represent a small data set) and/or inadequate understanding of the fragmentation.

The difference in intensity of $[M-H-HI]^-$ and $[M-H-HCl]^-$ was found to be significant using the Student-*t* test. The result supports the benzyne model for the production of $[M-H-HY]^-$ (Y = halogen) ions.

The accuracy of prediction clearly depends on our understanding the processes responsible for fragmentation of OP compounds, the extent of the data base, and the reproducibility of the spectra. Table 6 reveals that the positive and negative LMS from two of the five compounds (iodofenphos and dialifor) were predicted without error. One compound (phosalone) had only one intensity error in the negative ion LMS prediction, while the positive ion spectrum was predicted accurately. The remaining predictions contained few errors reflecting moieties not represented in the original data base, compounds **1**–**20**.

4. CONCLUSIONS

The laser mass spectra obtained from OP compounds depend on

Table 6 Predicted and observed fragments for five OP pesticides studied with laser mass spectrometry[a]

	Coumaphos		*Iodofenphos*		*Ronnel*		*Dialifor*		*Phosalone*	
Compound no.	**21**		**22**		**23**		**24**		**25**	
M.W.	362		412		330		393		367	
Mass range studied	*m/z* 135–750		*m/z* 105–850		*m/z* 100–650		*m/z* 100–800		*m/z* 100–800	
Predicted	*Predicted relative intensity*	*Observed relative intensity*	*Predicted relative intensity*	*Observed relative intensity*	*Predicted relative intensity*	*Observed relative intensity*	*Predicted relative intensity*	*Observed relative intensity*	*Predicted relative intensity*	*Observed relative intensity*
Positive ions										
M+H	64±34	50±18	<2	0.5±0.5	<2	0		N/A		N/A
M−R	30±16	25±10		N/A		N/A		N/A		N/A
M−Cl	10± 5	10± 4	1± 1	1± 1	1± 1	1± 1		N/A		N/A
M−RO	20±10[c]	0[c]	20±10	15± 8	20±10	5± 5		N/A		N/A
M−OZ	20±10[c]	100±30[c]	100± 0	100± 0	100± 0	50±50		N/A		N/A
M−SZ	10± 8	15± 6	16± 5	12± 4		N/A	5± 5	5± 5	5± 5	5± 5
OZ+2H	100±41	82±28		N/A		N/A		N/A		N/A
SZ+2H	4± 4	3± 1		N/A		N/A		N/A		N/A
M+H−CH_3Cl[b]	0	10± 4[c]		N/A		N/A		N/A		N/A
M+R		N/A	2± 2	7± 7		N/A	5± 5	0	5± 5	4± 4
M+H[c]		N/A		N/A	2± 2[c]	100±30[c]		N/A		N/A
M−SZ[c]		N/A		N/A	16± 8[c]	3± 3[c]		N/A		N/A
M+Z		N/A		N/A		N/A	20± 6	13± 5	20± 6	13± 5

Table 6 (continued)

	Coumaphos	*Idofenphos*	*Ronnel*	*Dialifor*	*Phosalone*
Compound no.	**21**	**22**	**23**	**24**	**25**
M+H−2CO	N/A	N/A	N/A	0.5±0.5 0	0.5±0.5 0
Z	N/A	N/A	N/A	100 ±0 100±0	100 ±0 100±0
PhCN	N/A	N/A	N/A	1 ±1 2±2	1 ±1 1±1
Negative ions					
M−H	5± 5 5±5	0.5± 0.5 0	0.5± 0.5 0	0.5±0.5 0.5+0.5	0.5±0.5 1±1
M−R	22±13 18±12	50 ±45 0	50 ±45[c] 5± 5[c]	1 ±1 1 ±1	1 ±1 5±5
M−Z	100± 0[c] 5± 5[c]	100 ±41 100 ± 0	100±41 100± 0	N/A	N/A
OZ	37±18[c] 100± 0[c]	37 ±18 20± 7	37 ±18 40±19	100±0 100±0	100±0 100±0
SZ	6± 6 5± 5	6 ±5 2± 2	6 ±5[c] 12±10[c]	N/A	N/A
M−H−HCl	N/A	<10 2± 2[d]	10 ±5 5± 5	N/A	N/A
M−H−HI	N/A	15 ±8 12±10[d]	N/A	N/A	N/A
Z−CHCH$_2$Cl	N/A	N/A	N/A	10±5 0	N/A
Z−CH$_2$	N/A	N/A	N/A	N/A	10 ±5[c] 19±7[c]

[a]Values given are $\pm t(a, df)s_i N^{-1/2}$; $t(a/2, df)$ = Student-t critical value at confidence ($a/2$) and degrees of freedom (df), S_i = Standard deviation of peak intensity, N = Number of spectra taken ($N=6$ for predicted intensities, $N=8$ for observed intensities), $a/2=0.005$, $df=N-1$.

[b]This ion was not predicted to appear.

[c]The differences between predicted and observed relative intensities of these ions tested significant using Student-t criteria.

[d]The difference between observed relative intensity of [M−H−HCl] and [M−H−HI] was determined significant using a Student-t test.

small variations in molecular structure. This dependence results in varying fragmentation and fragment yield. The variations in the spectra are "logical" in a chemical sense; that is, the difference observed can be rationalized from basic principles of organic chemistry. Furthermore, the similarity in structure among many of the compounds studied allow the development of qualitative models to explain spectral variation between compounds. For example, the protonation site in chlorpyrifos is likely the hetero-nitrogen of the **Z** substituent based on the appearance of $[OZ-2H]^+$ and $[SZ+2H]^+$ for compounds **1–3**. In turn, these qualitative models are used to predict spectra of other OP compounds with accuracy comparable to the reproducibility of the spectra.

The ability to predict mass spectra depends on the availability of a data set representing all moieties of interest. The accuracy of prediction is also dependent on the accuracy of models that explain the processes responsible for fragmentation; therefore, prediction is an excellent method for testing our depth of understanding. We are continuing studies of OP compounds to develop methods to confirm the fragmentation models proposed.

References

1. T. Cairns, E. G. Siegmund, G. M. Doose and A. C. Oken, *Anal. Chem.* **57**(4), 572A–576A (1985).
2. J. B. Weber. In: *Fate of Organic Pesticides in the Aquatic Environment* (R. F. Gould, ed.) (American Chemical Society, Washington, DC, 1972), pp. 55–120.
3. United States Environmental Protection Agency, Health Effects Research Laboratory, Environmental Toxicology Division. *Manual of Analytical Methods for the Analysis of Pesticides in Humans and Environmental Samples* (R. R. Watts, ed.) (Research Triangle Park, NC, 1980), EPA-600/8-80-038.
4. J. J. Morelli and D. M. Hercules, *Anal. Chem.* **58**(7), 1294 (1986).
5. J. N. Damico, *J. Assoc. Off. Anal. Chem.* **49**(5), 1027 (1966).
6. Wiley/NBS Spectral Data Base on Magnetic Tape, Cornell University, Ithaca, NY 14850, USA.
7. H.-J. Stan and G. Kellner, *Biomed. Mass. Spec.* **11**(11), 483 (1982).
8. H.-J. Stan, *Z. Anal. Chem.* **287,** 104 (1977).
9. H. R. Schulten and S.-E. Sun, *Intern. J. Environ. Anal. Chem.* **10,** 247 (1981).
10. J. J. Morelli and D. M. Hercules. In: *Microbeam Analysis* (Microbeam Analysis Society, San Francisco Press, San Francisco, CA, 1984), pp. 15–18.
11. J. J. Morelli, M. Junack, A. Benninghoven and D. M. Hercules, 1986, unpublished results.
12. H. J. Heinen, S. Meier and H. Vogt, *Int. J. Mass Spec. Ion Phys.* **47,** 19 (1983).
13. F. P. Novak and D. M. Hercules, 1986, unpublished results.

14. Quality Assurance Division, U.S. Environmental Monitoring Systems Laboratory, Office of Research and Development, U.S. Environmental Protection Agency, *Analytical Reference Standards and Supplemental Data: The Pesticides and Industrial Chemicals Repository* (Las Vegas, NV 89114, 1984), EPA-600/4-84-082.
15. J. March, *Advanced Organic Chemistry: Reactions, Mechanisms and Structures* (McGraw-Hill, Inc., New York, 1977).
16. T. R. Fukuto and R. L. Metcalf, *J. Am. Chem. Soc.* **76,** 5103 (1954).
17. D. E. C. Corbridge, *Phosphorus: An Outline of its Chemistry, Biochemistry and Technology* (Elsevier, New York, 1978).
18. D. E. C. Corbridge. *The Structural Chemistry of Phosphorus* (Elsevier, New York, 1974).
19. F. P. Novak and D. M. Hercules, 1986, unpublished results.
20. D. M. Hercules, K. Balasanmugam, T. A. Dang and C. P. Li, *Anal. Chem.* **54,** 280A (1982).
21. J. F. Ready, *Effects of High-Power Laser Radiation* (Academic Press, New York, 1971).
22. D. Bouchu, *Phosph. and Sulf.* **17,** 173 (1983).
23. F. C. V. Larsson, S. O. Lawesson, J. Moller and G. Schroll, *Acta Chem. Scand.* **27**(3), 747 (1973).
24. F. W. Rollgen. In: *Ion Formation from Organic Solids* (A. Benninghoven, ed.) (Springer-Verlag, New York, 1983), pp. 2–13.